

**The role of the self-steepening effect in soliton compression due  
to cross-phase modulation by dispersive waves**

Sabrina Pickartz

submitted: April 9, 2019

Weierstrass Institute  
Mohrenstr. 39  
10117 Berlin  
Germany  
E-Mail: [sabrina.pickartz@wias-berlin.de](mailto:sabrina.pickartz@wias-berlin.de)

No. 2585  
Berlin 2019



---

2010 *Mathematics Subject Classification.* 78A60, 78M22.

2010 *Physics and Astronomy Classification Scheme.* 42.65.-k, 42.81.Dp, 42.65.Re, 05.45.Yv.

*Key words and phrases.* Ultrashort pulses, Pulse compression, Soliton, Optical event horizons.

I would like to thank U. Bandelow und Sh. Amiranashvili for helpful discussions.

Edited by  
Weierstraß-Institut für Angewandte Analysis und Stochastik (WIAS)  
Leibniz-Institut im Forschungsverbund Berlin e. V.  
Mohrenstraße 39  
10117 Berlin  
Germany

Fax: +49 30 20372-303  
E-Mail: [preprint@wias-berlin.de](mailto:preprint@wias-berlin.de)  
World Wide Web: <http://www.wias-berlin.de/>

# The role of the self-steepening effect in soliton compression due to cross-phase modulation by dispersive waves

Sabrina Pickartz

## Abstract

We consider the compression and amplification of an ultrashort soliton pulse through the interaction with a weaker velocity-matched dispersive wave, in the so-called optical event horizon regime. We demonstrate that in this interaction scheme the self-steepening effect plays the key role in producing a strong soliton compression. While the interaction between the two pulses is mediated through cross phase modulation, the self-steepening effect produces an energy exchange, which enhances soliton compression. We provide numerical results and an analytical expression for energy transfer and compression rate.

## 1 Introduction

We consider the compression and amplification of an ultrashort soliton pulse through the cross phase modulation (XPM) interaction with a weaker velocity-matched dispersive wave in nonlinear optical fibers. A soliton of high intensity creates a refractive index barrier at which a dispersive wave (DW) of lower intensity is fully or partially trapped and accelerated. In a soliton co-moving frame this looks like the reflection and transmission at a barrier, and it is accompanied by the according frequency conversion of the reflected wave. This kind of wave trapping was observed in various experiments [15, 14, 17, 22, 28, 1, 26], and it has been studied numerically in a variety of circumstances, e.g. trapping by a single soliton [11, 27], successive reflection at a continuously decelerated soliton [10, 12], or trapping between two solitons [29, 8]. The role of DW frequency conversion at a soliton barrier for the generation of new frequencies has been investigated numerically, especially to explain the appearance of certain frequencies in super-continua [25, 24, 9]. Within super-continuum generation it was also observed, that this soliton-DW interaction can have a strong impact on the evolution of the soliton [7]. All soliton parameters, e.g. its carrier frequency and peak power, can be manipulated in a predictable and controlled fashion by a suitably chosen DW [19, 20]. It is a particularly intriguing feature that a soliton can be influenced by a control pulse which is much lower in intensity, especially as examples were found in which the soliton experienced an up to seven-fold increase in peak power [4]. This kind of soliton amplification and manipulation has been investigated as an additional way of producing super-continua, [6, 5], and for the generation of rogue waves [2, 3, 23].

It has been established that the interaction is mediated by XPM between soliton and dispersive wave [7, 19]. Here we demonstrate that it is the influence of the self-steepening effect that is decisive for the magnitude of soliton compression. In short: XPM leads to an energy-conserving reshaping of the soliton. This reshaping is a purely parametric process. The soliton adiabatically adjusts its parameters to the slow changes imposed by the interaction with the second wave. The main message of the present work is that, contrary to prior perceptions, the effect of adiabatic compression alone is way too weak to explain the extreme soliton compression rates observed. As we will see, the self-steepening effect must be taken into account. It results in an energy exchange which generates considerably stronger changes of soliton parameters.

The paper is organized as follows. First we compare the typical picture of soliton compression through XPM to a case in which the self-steepening is artificially switched off and the soliton compression is consequently weakened. In section 2 we give corresponding numerical simulation results. A model for the velocity-matched soliton-DW interaction scheme was established in [19], which we adjust to both settings, with and without self-steepening. We can then give an analytical expression the evolution of soliton peak power and pulse energy.

## 2 Soliton-DW interaction

A direct comparison of numerical simulations with and without self-steepening reveal the difference between the two scenarios. We numerically solve the generalized nonlinear Schrödinger equation

$$i\psi_z + D(i\partial_\tau)\psi + \gamma_0 [1 + i\eta_0\partial_\tau] |\psi|^2 \psi = 0. \quad (1)$$

It describes the propagation of the field envelope  $\psi = \psi(z, \tau)$  along an optical fiber, where  $z$  is the propagation distance,  $\tau = t - z\beta'(\omega_0)$  the retarded time. The dispersion operator is defined by  $D(i\partial_\tau)\psi(z, \tau) = \mathcal{F}^{-1}(D(\omega)\hat{\psi}(z, \omega))$  through Fourier transform of the dispersion function

$$D(\Delta\omega) = \beta(\omega_0 + \Delta\omega) - \beta(\omega_0) - \beta'(\omega_0) \Delta\omega. \quad (2)$$

The nonlinear parameter  $\gamma_0$ , and the self-steepening parameter  $\eta_0 = 1/\omega_0$  are each evaluated at reference frequency  $\omega_0$ . To observe the interaction of interest, we use the initial envelope

$$\psi(0, \tau) = \frac{\sqrt{P_0}}{\cosh\left(\frac{\tau - \tau_0}{\sigma_0}\right)} + \frac{\sqrt{P_1} e^{-i[\omega_{\text{DW}} - \omega_0]\tau}}{\cosh\left(\frac{\tau - \tau_1}{\sigma_1}\right)}.$$

The soliton has initial carrier frequency  $\omega_0$ , initial peak power  $P_0$ , initial duration  $\sigma_0$ , and initial delay  $\tau_0 = 0$ . The DW has initial carrier frequency  $\omega_{\text{DW}}$ , peak power  $P_1$ , and duration  $\sigma_1$ . Soliton and DW are velocity matched, meaning we can find frequencies  $\omega_0$  and  $\omega_1$  lying in opposite dispersion regimes yet with equal group velocities,  $\beta'(\omega_0) = \beta'(\omega_1)$ . The initial DW frequency is  $\omega_{\text{DW}} = \omega_1 + \Delta$ , with a small initial frequency offset  $\Delta$ . Only for small enough values of  $\Delta$  soliton and DW will interact. The specific range of an effective  $\Delta$ -interval was derived in [20]. Furthermore the initial DW peak power  $P_1$  is chosen much below the initial soliton peak power  $P_0$ . These conditions are necessary for the adiabatic soliton-feeding effect seen in Figure 4.

Figure 1 shows the typical interaction picture of soliton compression by a DW. The DW approaches the soliton, and is reflected in the co-moving frame. During this reflection process, the soliton is accelerated, which is recognized by the deflection of its trajectory in the temporal domain. In the shown example the soliton is compressed, its peak power multiplies almost 4-fold. In the spectral domain, we can see the soliton's frequency upshift and broadening of the spectral envelope, and the frequency conversion of the reflected DW.

Figure 2 shows the numerical solution of (1) with self-steepening artificially switched off using the same set of initial parameters as used in Figure 1. The soliton still traps parts of the approaching DW, yet becomes transparent very soon. The soliton is slightly accelerated, and its peak power multiplies by a mere factor 1.2. So the typical traits of the interaction are retained, but are much less pronounced.

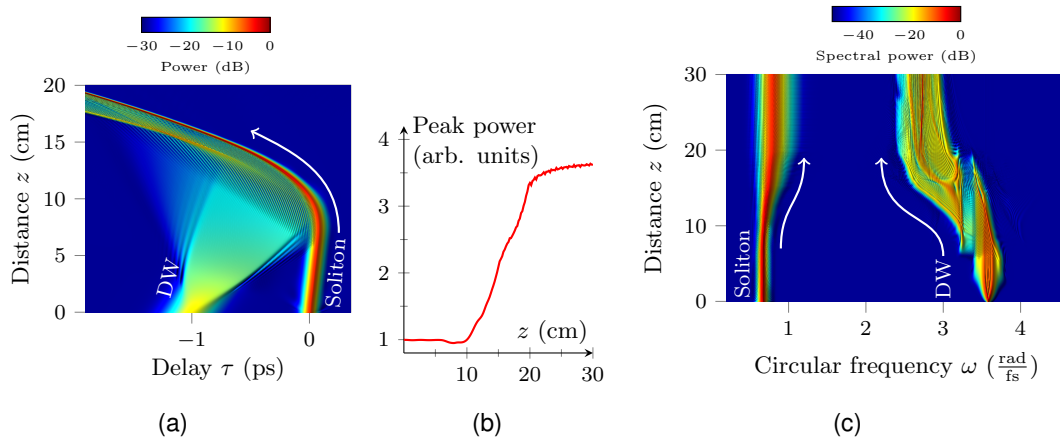


Figure 1: Interaction of soliton ( $\omega_0 = 0.67 \text{ rad fs}^{-1}$ ,  $\sigma_0 = 30 \text{ fs}$ ) and DW ( $\omega_1 = 3.586 \text{ rad fs}^{-1}$ ,  $\sigma_1 = 100 \text{ fs}$ , initially 25% of initial soliton peak power) in silica fiber. (a) In temporal domain the DW is reflected at the soliton, which is then deflected. (b) Soliton peak power multiplies by a factor 3.5. (c) Solitons frequency is up-shifted, and the DW frequency is converted down during the reflection process.

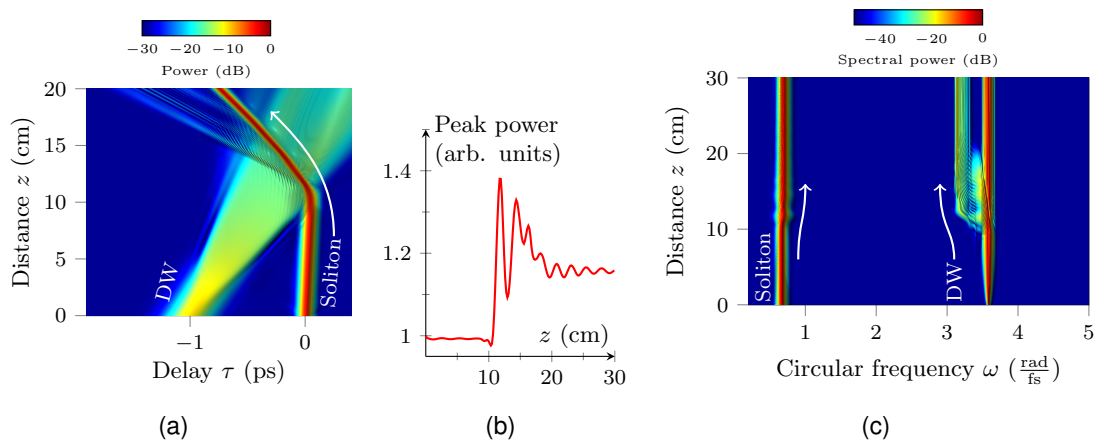


Figure 2: Interaction of soliton and DW in silica fiber. The same initial values as is Figure 1, yet the GNLS equation (1) is numerically solved with self-steepening artificially switched off ( $\eta_0 \equiv 0$ ). (a) The DW is still partially reflected at the soliton. (b) The soliton is only slightly compressed, its peak power amplifies by only a factor 1.2. (c) The upshift in soliton frequency is very small. We can see the frequencies of incoming and transmitted parts of the DW and the down-converted frequency of the reflected DW parts.

### 3 Model equations for soliton-DW interaction (Recap)

Here we briefly recap the analytical description of the soliton-DW interaction, which was first introduced in [19]. The model can be adapted to provide explicit expressions for soliton peak power and pulse energy depending on propagation distance, for either of the two scenarios with and without self-steepening.

The model is derived on the basis of two coupled NLS equations for the envelopes  $\psi$  and  $\psi_{\text{DW}}$  of soliton and DW, respectively:

$$i\partial_z\psi + D(i\partial_\tau)\psi + \gamma_0 [|\psi|^2 + 2|\psi_{\text{DW}}|^2] \psi = 0 \quad (3)$$

$$i\partial_z\psi_{\text{DW}} - \frac{\beta_1''}{2}\partial_\tau^2\psi_{\text{DW}} + \gamma_1 [|\psi_{\text{DW}}|^2 + 2|\psi|^2] \psi_{\text{DW}} = 0 \quad (4)$$

The equations are evaluated at the initial soliton frequency  $\omega_0$ , and the velocity matched frequency  $\omega_1$ . Thus both equations can use the retarded time  $\tau$  defining a frame co-moving with the initial soliton group velocity,  $v_g = 1/\beta'(\omega_0) = 1/\beta'(\omega_1)$ . The frequency offset  $\Delta$  from  $\omega_1$  is hidden in the initial condition of the DW envelope. Note that the soliton equation (3) must contain higher order dispersion terms to reflect the steep anomalous dispersion profile.

Equations (3) and (4) are solved analytically by different means. The soliton equation (3) is rearranged as perturbed NLS equation in which the XPM by the DW is treated as a perturbation, while the DW equation (4) is treated as a scattering problem of a plane wave reflected and transmitted at a solitonic barrier. The key to the success of the presented model lies in a generalization of the soliton perturbation theory which allows all material parameters to adapt to a changing soliton carrier frequency.

#### 3.1 Setup

The soliton equation (3) is rearranged as perturbed standard NLS equation:

$$i\partial_z\psi - \frac{\beta_0''}{2}\partial_\tau^2\psi + \gamma_0 |\psi|^2 \psi = iF, \quad (5)$$

where the higher order dispersion and XPM terms are gathered in the perturbation term

$$F = F(\psi, \psi^*, \psi_{\text{DW}}, \psi_{\text{DW}}^*) = i \sum_{m=3}^M \frac{\beta_0^{(m)}}{m!} [i\partial_\tau]^m \psi + i2\gamma_0 |\psi_{\text{DW}}|^2 \psi. \quad (6)$$

This is based on the assumption that the soliton reacts to small changes in its environment and adapts to it while retaining its soliton character. The unperturbed NLS equation (5) ( $F \equiv 0$ ) can be derived from the Lagrangian

$$\mathcal{L}_{\text{NLS}} = \frac{i}{2} \left[ \psi^* \frac{\partial\psi}{\partial z} - \psi \frac{\partial\psi^*}{\partial z} \right] + \frac{\gamma_0}{2} |\psi|^4 - \frac{\beta_0''}{2} \left| \frac{\partial\psi}{\partial\tau} \right|^2$$

by means of the variational derivative  $\frac{\delta}{\delta\psi^*} \mathcal{L}_{\text{NLS}} = 0$ . A variational approximation of the soliton envelope is calculated by stating an ansatz function, e.g.

$$\psi_0(z, \tau) = \frac{1}{\sigma} \sqrt{\frac{|\beta_0''|}{\gamma_0}} \frac{\exp(-i\nu [\tau - \tau_s] + i\theta)}{\cosh\left(\frac{\tau - \tau_s}{\sigma}\right)} \quad (7)$$

and integrating  $\mathcal{L}(\psi_0)$  over  $\tau$ . The resulting effective Lagrangian  $L_{\text{eff}} = - \left[ \nu \frac{d\tau_s}{dz} + \frac{d\theta}{dz} \right] \frac{2\beta_0''}{\gamma_0\sigma} - \frac{[\beta_0'']^2 \nu^2}{\gamma_0\sigma} + \frac{[\beta_0''']^2}{3\gamma_0\sigma^3}$  is a function of the  $z$ -dependent free soliton parameters, i.e. soliton duration  $\sigma(z)$ , frequency shift  $\nu(z)$ , time delay  $\tau_s(z)$  and phase  $\theta(z)$ . Variational derivatives by the soliton parameters result in a set of ordinary differential equations describing in total the evolution of soliton envelope (7). For example  $\frac{\delta L_{\text{eff}}}{\delta\theta} = 0$  results in the energy conservation  $\frac{d\mathcal{E}}{dz} = 0$ .

The influence of a non-vanishing perturbation onto the evolution of the soliton parameters can be calculated to be

$$\frac{\delta L_{\text{eff}}}{\delta r_j} = -2 \int d\tau \text{Im} \left( F \frac{\partial \psi_0^*}{\partial r_j} \right) \quad (8)$$

for any soliton parameter  $r_j = \sigma, \nu, \tau_s, \theta$  (cf. [13]).

The solution of equation (4) provides an explicit expression for  $\psi_{\text{DW}}(z, \tau)$  which can be used directly in the perturbation term  $F$  of the solitons equation. Assuming that the DW is of much lower intensity compared to the soliton, equation (4) can be linearized, and higher order dispersion and nonlinear phenomena can be ignored as they do not affect a low-intensity monochromatic DW. The soliton ansatz (7) is plugged in, so that it can be solved as the scattering of a plain wave at a soliton barrier. We get not only an analytical expression for  $\psi_{\text{DW}}$ , but also reflection and transmission coefficients depending on the changing soliton parameters.

### 3.2 Adaptation to varying soliton frequency

The way the soliton equation is solved above is pretty much according to the standard soliton perturbation theory, e.g. [13]. Yet in fact, it will fail to predict any changes in the soliton amplitude, as has been pointed out before. A generalization of the standard perturbation theory was introduced [19]. This generalization uses a perturbation equation in which all coefficients are functions depending on the varying soliton frequency

$$\omega_s = \omega_0 + \nu(z).$$

This is not merely the key to a proper prediction of soliton amplitude changes, but it also allows a better understanding of the importance of the self-steepening effect in soliton compression, as we shall see shortly.

The new soliton envelope

$$\psi_s(z, \tau) = \psi_0 \exp \left( -i\nu(z)\tau + i \int_0^z D(\omega_0 + \nu(z')) dz' \right) \quad (9)$$

is introduced. When plugged into (3) it yields a new soliton equation

$$i\partial_z \psi_0 + \tau \left[ \frac{d\nu}{dz} \right] \psi_0 + i [\beta'(\omega_0 + \nu(z)) - \beta'(\omega_0)] \partial_\tau \psi_0 + \sum_{m=2}^M \frac{\beta^{(m)}(\omega_0 + \nu(z))}{m!} [i\partial_\tau]^m \psi_0 + \gamma_0 [|\psi_s|^2 + 2|\psi_{\text{DW}}|^2] = 0. \quad (10)$$

To derive (10) first the following property of the dispersion operator was used:

$$D(i\partial_\tau) [\psi_0 e^{-i\nu\tau}] = e^{-i\nu\tau} D(\nu + i\partial_\tau) \psi_0. \quad (11)$$

Then the dispersion operator is expanded around  $\nu$ :

$$D(i\partial_\tau + \nu) = \sum_{m \geq 0} \frac{D^{(m)}(\nu)}{m!} [i\partial_\tau]^m \quad (12)$$

and rewritten in terms of the propagation constant  $\beta$  according to (2). The dispersion coefficients are now dependent on the soliton frequency shift  $\nu(z)$ . Because the dispersion coefficients, especially the GVD coefficient, are now evaluated accurately at any soliton frequency  $\omega_0 + \nu$ , the higher order dispersion terms become less important in the new equation. It is sufficient to set  $M = 4$ .

The introduction of the additional shift  $\nu$  is mathematically equivalent to the introduction of an accelerated coordinate system in quantum mechanics [16], hence the new term involving  $d\nu/dz$  appears in (10).

For the new soliton equation we can now evaluate a variational approximation of the soliton envelope  $\psi_0$ . Equation (10) is again reformulated as perturbation equation

$$\begin{aligned} i\partial_z \psi_0 + i[\beta'(\omega_0 + \nu(z)) - \beta'(\omega_0)] \partial_\tau \psi_0 \\ - \frac{\beta''(\omega_0 + \nu(z))}{2} \partial_\tau^2 \psi_0 + \gamma_0 |\psi_0|^2 \psi_0 + \tau \frac{d\nu}{dz} \psi_0 = iF \end{aligned} \quad (13)$$

in which higher order dispersion and XPM terms are collected into a perturbation function

$$F(\psi_0, \psi_{\text{bw}}) = i \sum_{m=3}^4 \frac{\beta^{(m)}(\omega_0 + \nu(z))}{m!} [i\partial_\tau]^m \psi_0 + i2\gamma_0 |\psi_{\text{bw}}|^2 \psi_0. \quad (14)$$

The Lagrangian

$$\begin{aligned} \mathcal{L}_{\text{Eq.(13)}} = \frac{i}{2} \left[ \psi^* \frac{\partial \psi}{\partial z} - \psi \frac{\partial \psi^*}{\partial z} \right] + \tau \frac{d\nu}{dz} |\psi|^2 \\ + \frac{i}{2} [\beta'(\omega_0 + \nu(z)) - \beta'(\omega_0)] \left[ \psi^* \frac{\partial \psi}{\partial \tau} - \psi \frac{\partial \psi^*}{\partial \tau} \right] \\ - \frac{\beta''(\omega_0 + \nu(z))}{2} \left| \frac{\partial \psi}{\partial \tau} \right|^2 + \frac{\gamma_0}{2} |\psi|^4. \end{aligned} \quad (15)$$

reproduces unperturbed equation (13). Given a suitable soliton ansatz function

$$\psi_0(z, \tau) = \frac{1}{\sigma} \sqrt{\frac{|\beta''(\omega_0 + \nu)|}{\gamma_0}} \frac{\exp(i\theta)}{\cosh \frac{\tau - \tau_s}{\sigma}}, \quad (16)$$

the procedure explained in the previous section can be directly applied to derive evolution equations for the soliton parameters.

## 4 Adiabatic soliton compression

The soliton scheme outlined in the previous section is here used to predict how the soliton evolves along the fiber with self-steepening ignored. We are interested primarily in the soliton's compression rate, therefore we focus on prediction of soliton duration and peak power. Equation (8) with variational derivative by  $\theta$  results in

$$\frac{d}{dz} \left[ \frac{1}{\sigma} \frac{\beta''(\omega_0 + \nu)}{\gamma_0} \right] = \int_{-\infty}^{\infty} d\tau \text{Re}(F\psi_0^*) = 0. \quad (17)$$

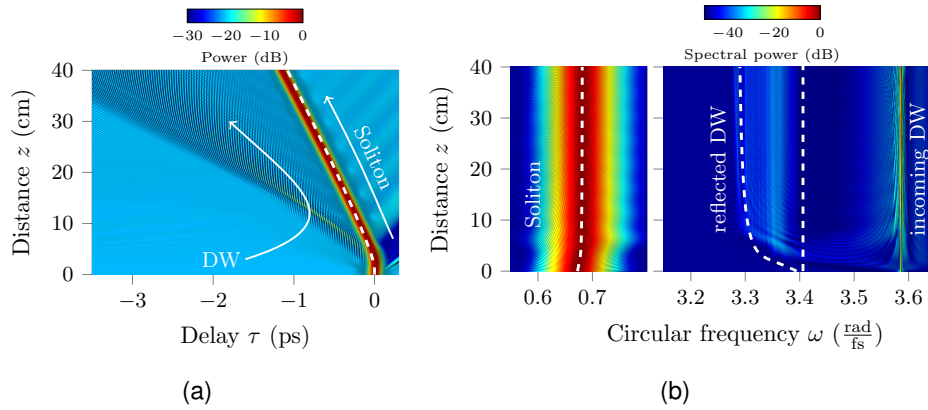


Figure 3: Interaction of a soliton ( $\omega_0 = 0.67 \text{ rad fs}^{-1}$ ,  $\sigma_0 = 40 \text{ fs}$ ) with a continuous DW ( $\Delta = 0.1 \text{ rad fs}^{-1}$ , and 1% initial soliton peak power), if self-steepening is ignored. Comparison of numerical and analytical results in temporal domain (a) and spectral domain (b). White dashed lines indicate predictions by the model equations, cf. [18].

The right hand side of the equation evaluates to zero for the given perturbation (14). It provides a simple relation for the change in soliton duration

$$\frac{\sigma(z)}{\sigma(0)} = \frac{\beta''(\omega_0 + \nu(z))}{\beta''(\omega_0)}. \quad (18)$$

Thus peak power  $P_s(z)/P_s(0) = \beta''(\omega_0)/\beta''(\omega_0 + \nu(z))$  only changes adiabatically due to a shifted carrier frequency. As there should be no energy exchange between soliton and DW through XPM, the soliton is expected to be unchanged. Consistent with this expectation the adiabatic model predicts soliton energy to be preserved:

$$\frac{\mathcal{E}_s(z)}{\mathcal{E}_s(0)} = \frac{\sigma(0)}{\sigma(z)} \frac{\beta''(\omega_0 + \nu(z))}{\beta''(\omega_0)} = 1. \quad (19)$$

The energy  $\mathcal{E}_s = \int |\psi_0(z, \tau')|^2 d\tau' = \frac{2}{\sigma} \frac{|\beta''(\omega_0 + \nu)|}{\gamma_0}$  is calculated using the soliton ansatz function.

Figure 3 shows the numerical solution to the NLS equation (1) with  $\eta_0 \equiv 0$  and initial condition

$$\psi(0, \tau) = \frac{\sqrt{P_0}}{\cosh\left(\frac{\tau - \tau_0}{\sigma_0}\right)} + \sqrt{P_1} e^{-i[\omega_{\text{DW}} - \omega_0]\tau}.$$

The continuous DW is initially fully reflected at the soliton barrier, yet only after about 5 cm of propagation the soliton becomes transparent to the DW. Soliton peak power only increases minimally. The dashed lines resulting from the adiabatic model equations are in good agreement with the numerical results.

## 5 Effect of self-steepening on soliton-DW interaction

The soliton behavior changes drastically when the self-steepening term is included into the calculations. To that end the self steepening term is introduced into the soliton equation (3),

$$i\partial_z \psi + D(i\partial_\tau) \psi + \gamma_0 [1 + i\eta_0 \partial_\tau] [|\psi|^2 + 2|\psi_{\text{DW}}|^2] \psi = 0.$$

The introduction of the new soliton envelope (9) produced  $z$ -dependent dispersion coefficients. The extra derivative by  $\tau$  of the self-steepening term applied to the new envelope results in a nonlinear coefficient which is also dependent on  $z$ :

$$\begin{aligned} \gamma_0 [1 + i\eta_0 \partial_\tau] [\psi_0(z, \tau) e^{-i\nu(z)\tau}] &= \frac{n_{2,0}\omega_0}{c} \left[ 1 + \frac{i}{\omega_0} \partial_\tau \right] [\psi_0(z, \tau) e^{-i\nu(z)\tau}] \\ &= e^{-i\nu(z)\tau} \frac{n_{2,0}[\omega_0 + \nu]}{c} \left[ 1 + \frac{i}{\omega_0 + \nu} \partial_\tau \right] \psi_0(z, \tau) \end{aligned}$$

All additional terms are collected in the perturbation function:

$$\begin{aligned} F(\psi_0, \psi_{\text{DW}}) &= i \sum_{m=3}^4 \frac{\beta^{(m)}(\omega_0 + \nu)}{m!} [i\partial_\tau]^m \psi_0 \\ &\quad - \gamma_s \eta_s \partial_\tau [|\psi_0|^2 \psi_0] + i2\gamma_s [1 + i\eta_s \partial_\tau] [|\psi_{\text{DW}}|^2 \psi_0] \end{aligned} \quad (20)$$

with nonlinear and self-steepening coefficients

$$\gamma_s(z) = \frac{n_{2,0}[\omega_0 + \nu(z)]}{c}, \quad (21)$$

$$\eta_s(z) = 1/[\omega_0 + \nu(z)]. \quad (22)$$

For this perturbation function, equation (8) with variational derivatives by  $\theta$  and  $\tau_s$  results in the following two ordinary differential equations for soliton duration:

$$\frac{d}{dz} \left[ \frac{\beta''(\omega_0 + \nu)}{\sigma \gamma_s} \right] = -2\eta_s \frac{\beta''(\omega_0 + \nu)}{\sigma^3} \int d\tau \frac{\tanh \frac{\tau - \tau_s}{\sigma}}{\cosh^2 \frac{\tau - \tau_s}{\sigma}} |\psi_{\text{DW}}(z, \tau)|^2 \quad (23)$$

and frequency shift:

$$\frac{d\nu}{dz} = -\frac{2\gamma_s}{\sigma^2} \int d\tau \frac{\tanh \frac{\tau - \tau_s}{\sigma}}{\cosh^2 \frac{\tau - \tau_s}{\sigma}} |\psi_{\text{DW}}(z, \tau)|^2. \quad (24)$$

Independent of the explicit form of  $\psi_{\text{DW}}$  both equations can be combined to

$$\frac{d}{dz} \left[ \frac{\beta''(\omega_0 + \nu)}{\sigma \gamma_s} \right] = \frac{\beta''(\omega_0 + \nu)}{\sigma \gamma_s} \eta_s \frac{d\nu}{dz} \quad (25)$$

and integrated. This results in an explicit expression for soliton duration  $\sigma$  as a function of frequency shift  $\nu$ :

$$\frac{\sigma(z)}{\sigma(0)} = \frac{\beta''(\omega_0 + \nu(z))}{\beta''(\omega_0)} \frac{\gamma_s(0) \eta_s(z)}{\gamma_s(z) \eta_s(0)} = \frac{\beta''(\omega_0 + \nu(z))}{\beta''(\omega_0)} \left[ 1 + \frac{\nu(z)}{\omega_0} \right]^{-2}. \quad (26)$$

Also soliton peak power changes no longer just adiabatically:

$$\frac{P_s(z)}{P_s(0)} = \left[ \frac{\sigma(0)}{\sigma(z)} \right]^2 \frac{\gamma_s(0) \beta''(\omega_0 + \nu(z))}{\gamma_s(z) \beta''(\omega_0)} = \left[ 1 + \frac{\nu(z)}{\omega_0} \right]^3 \frac{\beta''(\omega_0)}{\beta''(\omega_0 + \nu(z))}. \quad (27)$$

and the soliton energy now changes with  $z$ :

$$\frac{\mathcal{E}_s(z)}{\mathcal{E}_s(0)} = \frac{\sigma(0) \beta''(\omega_0 + \nu(z))}{\sigma(z) \beta''(\omega_0)} = 1 + \frac{\nu(z)}{\omega_0}. \quad (28)$$

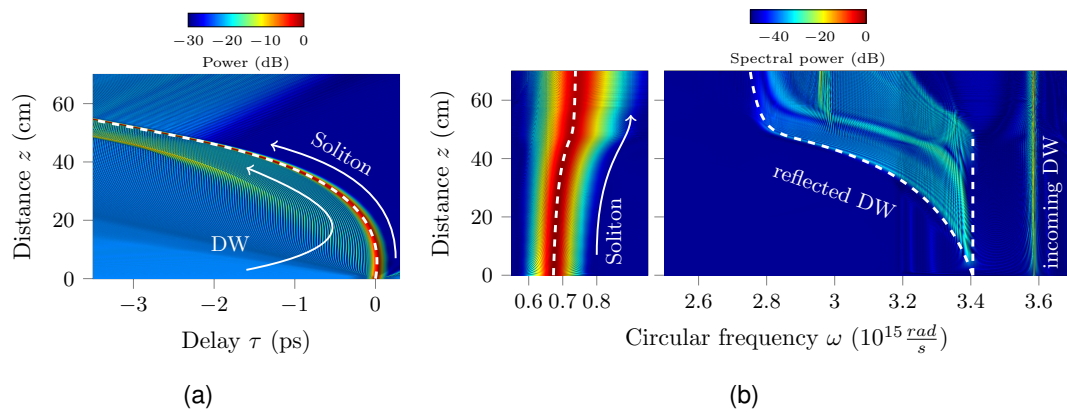


Figure 4: Interaction of a soliton with a continuous DW for the same initial values as used in Figure 3, yet here self-steepening is taken into account. Comparison of numerical and analytical results in temporal domain (a) and in spectral domain (b). White dashed lines indicate predictions by the model equations, cf. [18].

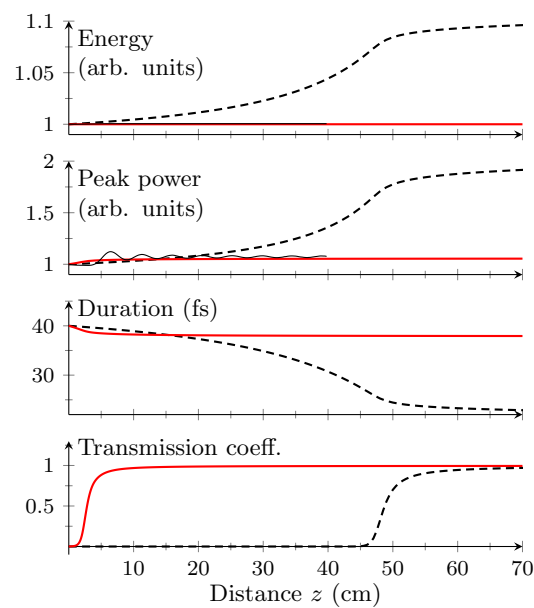


Figure 5: Evolution of soliton parameters are compared for the examples shown in Figures 3 and 4. Thick red lines result from model equation derived ignoring the self-steepening term; thin solid black lines are the result of the according numerical simulation of GNLSE. Dashed black lines result from model equations including the self-steepening term. The soliton is only effectively compressed when self-steepening is taken into account, cf. [18].

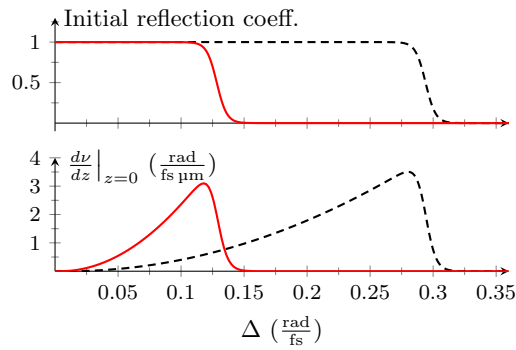


Figure 6: The top frame shows the possible range of DW frequencies which are initially reflected at a soliton with  $\omega_0 = 0.67 \text{ rad fs}^{-1}$  and  $\sigma_0 = 40 \text{ fs}$ . The bottom frame shows the initial impact of a certain DW on the soliton. Red solid lines represent calculations ignoring self-steepening, black dashed lines result from those with self-steepening included. The disagreement is due to the artificially removed self-steepening term, cf. [18].

Figure 4 compares the results of these extended model equations with numerical solution to NLS equation (1). Initial values are the same in used in Figure 3. The DW is fully reflected for a much longer distance, only after about 50 cm the soliton becomes transparent. Again the agreement between model and numerics is quite accurate.

In Figure 5 the evolution of soliton parameters for the example shown in Figure 3 is directly compared to the results shown in 4 for the case with self-steepening ignored. Without self-steepening, the soliton energy stays unchanged. With self-steepening, the soliton only gains a small amount of energy, yet the gain in peak power heavily depends on this small increase in energy, as is confirmed by (27) and (28). Over the course of a much longer interaction length, the soliton's peak power almost doubles.

## 6 Result

It is not immediately apparent that the self-steepening effect should have a strong impact on either pulse, soliton or DW. Therefore it has often been neglected in investigations of soliton-DW interactions. If the focus lies on the evolution of the DW and the soliton is considered unchanged by the interaction, this may be justified, but one must bear in mind that the picture is incomplete, as it neglects the important implications of an energy exchange between the pulses. When the focus lies on the soliton compression or manipulation by a DW, self-steepening must be included into considerations. We have demonstrated the apparent difference in soliton compression for the two scenarios of included vs. ignored self-steepening effect. The expressions derived for the evolution of soliton peak power and energy confirm that the energy exchange between DW and soliton resulting from the self-steepening effect is a crucial factor in a strong soliton compression.

Figure 6 (top frame) shows the initial reflection coefficient versus initial DW frequencies for the initial soliton with carrier frequency  $\omega_0 = 0.67 \text{ rad fs}^{-1}$  and duration  $\sigma_0 = 40 \text{ fs}$ . The DW frequency should be chosen, such that the DW is initially fully reflected. For a given soliton, the plotted reflection coefficient determines the DW frequency interval, which will result in an effective interaction. Another option is to evaluate the righthand side the frequency ODEs (24) at the beginning of the fiber for varying DW frequencies. The resulting curve is shown in Figure 6 (bottom frame). The curve shows the DW frequency interval of interaction, which coincides with the frequency interval predicted by the reflection coefficient (top frame). The shape of the curve should indicate how strong the soliton is initially

affected by a DW of a certain frequency. At the peaks of the curve the strongest initial effect on the soliton should be found. Looking at the interaction interval, it is clear, that the range of possible DW frequencies for an effective interaction is much smaller if self-steepening is ignored. These findings confirm again that the self-steepening term plays an essential role in a possibly strong impact on soliton evolution. The model for soliton feeding by dispersive waves proves to be robust and versatile, as it is easily adjusted to accurately predict evolution behavior from the simple interaction schemes of pure XPM interaction focussing on the DW, to situations in which self-steepening results in strong soliton compression. Even the effect of Raman scattering can be described in a straight forward manner [21].

## References

- [1] A. Choudhary and F. König. Efficient frequency shifting of dispersive waves at solitons. *Optics Express*, 20(5):5538–5546, 2012.
- [2] A. Demircan, S. Amiranashvili, C. Brée, C. Mahnke, F. Mitschke, and G. Steinmeyer. Rogue events in the group velocity horizon. *Scientific Reports*, 2(850), 2012.
- [3] A. Demircan, S. Amiranashvili, C. Brée, C. Mahnke, F. Mitschke, and G. Steinmeyer. Rogue wave formation by accelerated solitons at an optical event horizon. *Applied Physics B*, 115(3):343–354, 2014.
- [4] A. Demircan, S. Amiranashvili, C. Brée, U. Morgner, and G. Steinmeyer. Adjustable pulse compression scheme for generation of few-cycle pulses in the midinfrared. *Optics Letters*, 39(9):2735–2738, 2014.
- [5] A. Demircan, S. Amiranashvili, C. Brée, U. Morgner, and G. Steinmeyer. Supercontinuum generation by multiple scatterings at a group velocity horizon. *Optics Express*, 22(4):3866–3879, 2014.
- [6] A. Demircan, S. Amiranashvili, C. Brée, and G. Steinmeyer. Compressible octave spanning supercontinuum generation by two-pulse collisions. *Physical Review Letters*, 110(23):233901, 2013.
- [7] A. Demircan, S. Amiranashvili, and G. Steinmeyer. Controlling light by light with an optical event horizon. *Physical Review Letters*, 106:163901, 2011.
- [8] Z. Deng, X. Fu, J. Liu, C. Zhao, and S. Wen. Trapping and controlling the dispersive wave within a solitonic well. *Optics Express*, 24(10):10302, 2016.
- [9] R. Driben, F. Mitschke, and N. Zhavoronkov. Cascaded interactions between raman induced solitons and dispersive waves in photonic crystal fibers at the advanced stage of supercontinuum generation. *Optics Express*, 18(25):25993, 2010.
- [10] A. V. Gorbach and D. V. Skryabin. Bouncing of a dispersive pulse on an accelerating soliton and stepwise frequency conversion in optical fibers. *Optics Express*, 15(22):14560, 2007.
- [11] A. V. Gorbach and D. V. Skryabin. Light trapping in gravity-like potentials and expansion of supercontinuum spectra in photonic-crystal fibres. *Nature Photonics*, 1(11):653–657, 2007.

- [12] A. V. Gorbach and D. V. Skryabin. Theory of radiation trapping by the accelerating solitons in optical fibers. *Physical Review A*, 76(5), 2007.
- [13] A. Hasegawa and M. Matsumoto. *Optical Solitons in Fibers*. Springer, 3rd, rev. and enl. ed. edition, 2003.
- [14] N. Nishizawa and T. Goto. Characteristics of pulse trapping by use of ultrashort soliton pulses in optical fibers across the zero-dispersion wavelength. *Optics Express*, 10(21):1151–1159, 2002.
- [15] N. Nishizawa and T. Goto. Pulse trapping by ultrashort soliton pulses in optical fibers across zero-dispersion wavelength. *Optics Letters*, 27(3):152–154, 2002.
- [16] A. Peres. *Quantum Theory: Concepts and Methods*, volume 72 of *Fundamental Theories of Physics*. Kluwer, 2002.
- [17] T. G. Philbin, C. Kuklewicz, S. Robertson, S. Hill, F. König, and U. Leonhardt. Fiber-optical analog of the event horizon. *Science*, 319(5868):1367–1370, 2008.
- [18] S. Pickartz. *All-optical control of fiber solitons*. PhD thesis, Humboldt-Universität zu Berlin, Mathematisch-Naturwissenschaftliche Fakultät, 2018.
- [19] S. Pickartz, U. Bandelow, and S. Amiranashvili. Adiabatic theory of solitons fed by dispersive waves. *Physical Review A*, 94(3):033811/1–12, 2016.
- [20] S. Pickartz, U. Bandelow, and S. Amiranashvili. Efficient all-optical control of solitons. *Optical and Quantum Electronics*, 48(11):503/1–7, 2016.
- [21] S. Pickartz, C. Brée, U. Bandelow, and S. Amiranashvili. Cancellation of Raman self-frequency shift for compression of optical pulses. In *2017 International Conference on Numerical Simulation of Optoelectronic Devices (NUSOD)*. IEEE, 2017.
- [22] S. Robertson and U. Leonhardt. Frequency shifting at fiber-optical event horizons: The effect of Raman deceleration. *Physical Review A*, 81(6):063835, 2010.
- [23] M. F. Saleh, C. Conti, and F. Biancalana. Anderson localisation and optical-event horizons in rogue-soliton generation. *Optics Express*, 25(5):5457–5465, 2017.
- [24] D. V. Skryabin and A. V. Gorbach. Colloquium: Looking at a soliton through the prism of optical supercontinuum. *Reviews of Modern Physics*, 82(2):1287–1299, 2010.
- [25] D. V. Skryabin and A. V. Yulin. Theory of generation of new frequencies by mixing of solitons and dispersive waves in optical fibers. *Physical Review E*, 72(1), 2005.
- [26] L. Tartara. Frequency shifting of femtosecond pulses by reflection at solitons. *IEEE Journal of Quantum Electronics*, 48(11):1439–1442, 2012.
- [27] W. Wang, H. Yang, P. Tang, C. Zhao, and J. Gao. Soliton trapping of dispersive waves in photonic crystal fiber with two zero dispersive wavelengths. *Optics Express*, 21(9):11215, 2013.
- [28] K. E. Webb, M. Erkintalo, Y. Xu, N. G. R. Broderick, J. M. Dudley, G. Genty, and S. G. Murdoch. Nonlinear optics of fibre event horizons. *Nature Communications*, 5:4969 EP –, 2014.
- [29] A. V. Yulin, R. Driben, B. A. Malomed, and D. V. Skryabin. Soliton interaction mediated by cascaded four wave mixing with dispersive waves. *Optics Express*, 21(12):14481, 2013.